choice of reference system, are described. It is demonstrated how the MFP-axis formulation introduces singularities in the EOM. The singularities are identified, and the effect of their removal is shown in a numerical application. The conclusion is that the body-axis formulation generally leads to a more accurate solution.

As part of the current investigation, equations were derived for the steady-state limits of common motion variables. These limits are not affected by the various modeling techniques discussed here.

Acknowledgment

The author wishes to thank Daniel M. Ortega of the Boeing Phantom Works, Department of Loads and Dynamics, for generating the structural and aerodynamic data that were used in the sample problem.

References

[1]Winther, B. A., Goggin, P. J., and Dykman, J. R., "Reduced-Order Aeroelastic Model Development and Integration with Nonlinear Simulation," *Journal of Aircraft*, Vol. 37, No. 5, 2000, pp. 833–839.

[2]Albano, E., and Rodden, W. P., "A Doublet-Lattice Method for Calculating Lift Distributions on Oscillating Surfaces in Subsonic Flow," *AIAA Journal*, Vol. 7, No. 2, 1969, pp. 279–285.

[3]Giesing, J. P., Kalman, T. P., and Rodden, W. P., "Subsonic Unsteady Aerodynamics for General Configurations," U.S. Air Force Flight Dynamics Lab., Rept AFFDL-TR-71-5, Dayton, OH, Nov. 1971.

[4]Etkin, B., *Dynamics of Flight*, Wiley, New York, 1959, pp. 189–225.

[5]Rodden, W. P. (ed.), *MSC/NASTRAN Handbook for Aeroelastic Analysis*, MSR-57, MacNeal–Schwendler, Los Angeles, CA, Nov. 1987, Chaps. 8–10.

Extending Slender Wing Theory to Not So Slender Wings

Lance W. Traub*
Texas A&M University,
College Station, Texas 77843-3141

Nomenclature

AR	=	aspect ratio
a.c.	=	aerodynamic center
b	=	wing span
$b(x)$	=	local wing span
C_{Di}	=	induced drag coefficient
C_L	=	lift coefficient
$C_{L\alpha}$	=	lift-curve slope
$C_l(x)$	=	local lift coefficient
$Cm_{\text{l.e.}}$	=	wing apex pitching moment coefficient
Cr	=	root chord
C_T	=	leading-edge thrust coefficient
Kv	=	vortex lift constant
L	=	lift
$m(x)$	=	local apparent mass
S	=	wing area
U	=	freestream velocity
x, y	=	Cartesian coordinate
x_{cl}	=	location of wing's center of lift
α	=	angle of attack
α_i	=	induced angle of attack
ε	=	wing apex half angle
Λ	=	wing leading-edge sweep angle
ρ	=	density

Received 13 June 2002; revision received 16 October 2002; accepted for publication 18 October 2002.

*Texas Engineering Experiment Station Research Scientist/Lecturer, Aerospace Engineering Department. Associate Member AIAA.

Introduction

THE delta wing configuration has been extensively studied as a configuration that represents a realistic compromise between high-speed efficiency and low-speed maneuverability. The widespread adoption of this configuration in the late 1940s and 1950s promulgated the development of theoretical methods capable of predicting the behavior of these wings. Non-numerical efforts to predict the attached flow lift included slender wing theory (SWT)[1,2] and the method of Lawrence.[3] SWT was further developed by Lomax and Sluder[4] to account for the trailing-edge Kutta condition and compressibility. The resulting expressions compare reasonably with experiment[4] but are somewhat cumbersome, lacking the simplicity and ease of computation inherent in the original formulation. Similar observations can be made regarding the method of Lawrence.[3]

SWT[1,2] yields simple expressions to predict the lift, drag, and pitching moment coefficient of slender delta wings with fully attached leading-edge flow. However, the simplifications inherent in SWT limit its utility for wings with aspect ratios generally greater then 0.5, due to preclusion of trailing-edge effects. It is assumed that the chordwise velocity gradients are negligible such that the governing linearized partial differential equation transforms to Laplace's equation in a crossflow plane. Wing properties are evaluated in this cross flowplane that is assumed representative for all crossflow planes. As the wing extends to infinity chordwise, each crossflow plane is essentially a Trefftz plane. SWT predicts an elliptic spanwise load distribution. As chordwise effects are neglected in this methodology, the results are applicable for incompressible and compressible flow. The primary results from SWT are summarized as follows:

$$C_{L\alpha} = (\pi/2)\text{AR}, \qquad C_{Di} = C_L^2 \big/ \pi\,\text{AR} = (\pi/4)\text{AR}\alpha^2$$

$$\text{a.c.}/Cr = \tfrac{2}{3}, \qquad Cm_{\text{l.e.}} = -\pi\,\text{AR}\alpha/3$$

The simplicity of these equations makes them attractive for preliminary design use, as well as for educational purposes, as they can readily be committed to memory. However, their poor accuracy for the majority of practical delta wing configurations limits their utility. It would be useful for these applications to have similarly simple expressions that are applicable to a wider range of delta wings. In this Note, SWT is extended to include trailing-edge effects. Resulting expressions are compared with numerical and experimental data for validation.

Methodology

In the following analysis, it is assumed that the delta wings are planar and that their leading-edge flow is fully attached (100% leading-edge suction). The fluid is also assumed incompressible. Jones'[1] presentation of SWT relates the lift per unit chord of the wing to the rate of increase of the apparent mass of the fluid in a fixed axial crossflow plane as its penetrated by the wing. As the wing penetrates the plane, the scale of the flow increases, requiring a lift force equal to the downward velocity multiplied by the local increase of the additional apparent mass.[1] At any crossflow plane, the apparent mass of the fluid is given by

$$m(x) = \rho\pi b(x)^2/4 \tag{1}$$

Equation (1) represents the apparent mass for a falling flat plate, showing that the local fluid entrained consists of a cylinder with a diameter equal to that of the local wingspan. Consequently, $m(x)$ increases parabolically toward the trailing edge of the wing. The lift per unit chord is related to the apparent mass by [noting that $b(x) = 2x\tan(\varepsilon)$]

$$\frac{\mathrm{d}L}{\mathrm{d}x} = U^2\alpha\frac{\mathrm{d}m(x)}{\mathrm{d}x} = U^2\alpha\rho\pi\frac{2b(x)}{4}\frac{\mathrm{d}b(x)}{\mathrm{d}x} = U^2\alpha\rho 2\pi x\tan(\varepsilon)^2 \tag{2}$$

As such, the rate of change of the apparent mass and, hence, local lift varies linearly with chordwise distance. Equation (2) implies that if

the wing span is no longer increasing, for example, the tip sections of a cropped delta wing, the local lift is zero. From a vorticity perspective, this implies that at this location no spanwise vortex filaments exist; all filaments are streamwise and parallel to the freestream.

Mathematical simulation of a wing's trailing edge is achieved through imposition of the Kutta condition, inferring that the differential loading across the trailing edge is zero. The form of Eq. (2) suggests that a Kutta-type condition may be imposed by requiring that $\mathrm{d}m(x)/\mathrm{d}x$ (and so the local loading) tends to zero as the trailing edge is approached. This would physically imply that the presence of the trailing edge is indicated by the wing no longer increasing the scale of the flow as it penetrates the fixed crossflow plane, which is analogous to stating that all vortex filaments are streamwise. A modification to the form of $\mathrm{d}m(x)/\mathrm{d}x$ as presented in Eq. (2) may be assumed to be of the form

$$\frac{\mathrm{d}m(x)}{\mathrm{d}x} = \rho\pi \frac{b(x)}{2} \frac{\mathrm{d}b(x)}{\mathrm{d}x}\left[1 - \frac{x}{Cr}\sin(\varepsilon)\right] \tag{3}$$

Independently, the correction for trailing-edge effects $[1 - x/Cr\sin(\varepsilon)]$ represents a linear reduction in the rate of change of the apparent mass with the chord. Sweep dependence requires the incorporation of a function that eliminates trailing-edge effects for an infinite slender wing, that is, as $\varepsilon \to 0$ deg. A suitable function is a sinusoidal variation with ε as shown in Ref. 5, where the location of the wing's aerodynamic center (a.c.) is shown to be dependent on $\sin(\varepsilon)$. With the inclusion of sweep dependence, Eq. (3) no longer explicitly satisfies the Kutta condition at the wing's trailing edge (except for $\varepsilon = 90$ deg). A more complicated expression satisfying this condition would not be within the spirit of simplicity of the original theory, such that simple final relations would not result. However, Eq. (3) facilitates excellent predictions of loads and coefficients.

The local wingspan of a delta wing is given by

$$b(x) = 2x\tan(\varepsilon) \tag{4}$$

Substitution of Eq. (4) into Eq. (3) and evaluation yields

$$\frac{\mathrm{d}m(x)}{\mathrm{d}x} = 2\rho\pi\tan(\varepsilon)^2\left[x - \frac{x^2}{Cr}\sin(\varepsilon)\right] \tag{5}$$

The lift coefficient per unit length may be found by substitution of Eq. (5) into the definition for $\mathrm{d}L/\mathrm{d}x$ as presented by Eq. (2). Nondimensionalizing by the freestream dynamic pressure and local wing span yields [where $\mathrm{AR} = 4\tan(\varepsilon)$]

$$C_l(x) = [2\pi\tan(\varepsilon)\alpha/x][x - (x^2/Cr)\sin(\varepsilon)]$$

$$= (\pi\,\mathrm{AR}\alpha/2x)[x - (x^2/Cr)\sin(\varepsilon)] \tag{6}$$

and the chordwise loading is given by

$$C_l(x)(x/Cr) = 2\pi\tan(\varepsilon)\alpha[x/Cr - (x^2/Cr^2)\sin(\varepsilon)]$$

$$= (\pi\,\mathrm{AR}\alpha/2)[x/Cr - (x^2/Cr^2)\sin(\varepsilon)] \tag{7}$$

Although not included due to space limitations, comparison of Eq. (7) with the experimental data of Kirkpatrick[6] and a vortex lattice panel method[7] showed good agreement. The total lift of the wing follows as

$$L = \int_0^{Cr} \frac{\mathrm{d}L}{\mathrm{d}x}\,\mathrm{d}x = \int_0^{Cr} U^2\alpha\frac{\mathrm{d}m(x)}{\mathrm{d}x}\,\mathrm{d}x \tag{8}$$

Substitution of Eq. (5) into Eq. (8) gives

$$L = 2\rho\pi\tan(\varepsilon)^2\alpha U^2 Cr^2\left\{\tfrac{1}{2} - [\sin(\varepsilon)/3]\right\} \tag{9}$$

The lift coefficient follows, using $S = Cr^2\tan(\varepsilon)$ for a delta wing

$$C_L = L\Big/\tfrac{1}{2}\rho U^2 S = 4\pi\tan(\varepsilon)\alpha\left\{\tfrac{1}{2} - [\sin(\varepsilon)/3]\right\}$$

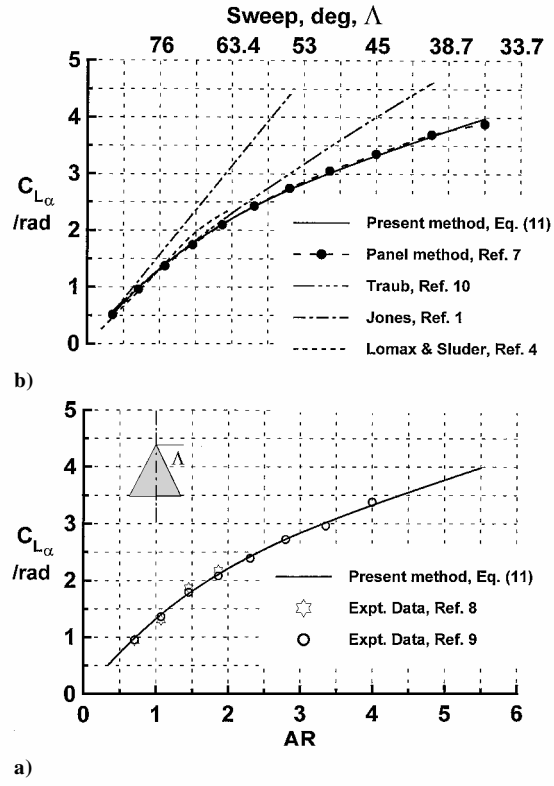

Fig. 1 Comparisons of predicted wing lift-curve slope a) with experimental data and b) with numerical and theoretical data.

which with $\mathrm{AR} = 4\tan(\varepsilon)$ gives

$$C_L = (\pi\,\mathrm{AR}\alpha/2)\{1 - [2\sin(\varepsilon)/3]\} \tag{10}$$

$$C_{L\alpha} = (\pi\,\mathrm{AR}/2)\{1 - [2\sin(\varepsilon)/3]\} \tag{11}$$

C_L may also be determined using Eq. (6) in concert with

$$C_L = \frac{2\tan(\varepsilon)}{S}\int_0^{Cr} xC_l(x)\,\mathrm{d}x$$

Equation (11) reduces to the slender wing result as $\varepsilon \to 0$ deg. Finite wing effects are indicated through the $[1 - 2\sin(\varepsilon)/3]$ term. Predictions using Eq. (11) with experimental data[8,9] are presented in Fig. 1a. The experimental data of Wentz and Kohlman[9] are widely used as a baseline for computational code validation and as such are regarded as representative. The presentation in Fig. 1a shows excellent agreement between the experimental data[8,9] and the predictions of Eq. (11).

Comparisons of Eq. (11) with computational and theoretical results for the lift-curve slope of thin delta wings are presented in Fig. 1b. The computational results were determined using the Lamar–Gloss[7] panel method. These, and all subsequent panel method data are denoted by solid circles to aid differentiation from the present predictions. Also indicated in Fig. 1b is a prediction using an approximation for $C_{L\alpha}$ derived using a Sychev similarity parameter (see Ref. 10), which is given by

$$C_{L\alpha} = 4\tan(\varepsilon)^{0.8} = \mathrm{AR}/\tan(\varepsilon)^{0.2} \tag{12}$$

Data from the method of Lomax and Sluder[4] are also included. Figure 1b shows that the current expression [Eq. (11)] yields excellent agreement with the numerical results, as does Eq. (12) for a more limited AR range. Equation (11) shows far better accuracy for high AR(>2) deltas then Eq. (12) and, as shown, provides predictions generally within 1% of the computational results for any likely practical delta wing of interest, a significant result given the simplicity of Eq. (11).

For slender wings, Jones[1] has shown that the attached flow spanwise loading is elliptical, a result also seen in numerical results. Thus, the inviscid drag for a planar delta wing with attached flow may be estimated as:

$$C_{Di} = C_L^2 \big/ \pi \mathrm{AR} = (\pi/4)\mathrm{AR}\alpha^2\left[1 - \tfrac{2}{3}\sin(\varepsilon)\right]^2 \qquad (13)$$

Under the assumption of elliptic loading, the induced angle of attack is readily determined as

$$\alpha_i = C_L/\pi \mathrm{AR} \qquad (14)$$

which on substitution of Eq. (10) yields

$$\alpha_i = (\alpha/2)\left(1 - \tfrac{2}{3}\sin(\varepsilon)\right) \qquad (15)$$

As $\varepsilon \to 0$ deg, Eq. (15) reduces to the classical result indicating that the resultant inviscid loading is inclined rearward at half the wing's geometric angle of attack. The location of the wing's center of lift may be found as follows:

$$Lx_{\mathrm{cl}} = \int_0^{Cr} \frac{\mathrm{d}L}{\mathrm{d}x} x \,\mathrm{d}x \qquad (16)$$

Substitution of Eq. (2) and Eq. (5) into Eq. (16) and integration yields

$$x_{\mathrm{cl}}/Cr = \left[\tfrac{1}{3} - \tfrac{1}{4}\sin(\varepsilon)\right] \big/ \left[\tfrac{1}{2} - \tfrac{1}{3}\sin(\varepsilon)\right] \qquad (17)$$

As $\varepsilon \to 0$ deg, Eq. (17) gives the slender wing result, that is $x_{\mathrm{cl}}/Cr = \frac{2}{3}$. As the wing is assumed to be thin and planar, Eq. (17) also corresponds to the location of the wing's a.c. Figure 2a presents comparisons of Eq. (17) with experimental data, the panel method, and an approximation given in Ref. 5. The data show good agreement, but indicate that the location of the wing's a.c. is predicted to be too far aft. This is a consequence of incomplete enforcement of the Kutta condition, resulting in excessive rear loading over the wing. The pitching moment about the wing's apex is also readily determined as

$$Cm_{\mathrm{l.e.}} = -C_L(x/Cr) = -\pi \mathrm{AR}\alpha\left[\tfrac{1}{3} - \tfrac{1}{4}\sin(\varepsilon)\right] \qquad (18)$$

Figure 2b presents predictions of $Cm_{\mathrm{l.e.}}$ using Eq. (18) with numerical and experimental data. The predictions show close accord with the numerical computations and experimental results. However, the moment is slightly larger than indicated by the panel method, once again reflecting the somewhat overestimated aft loading.

When fully attached flow and low α are assumed, the wing's leading-edge thrust (or inviscid axial force) may be estimated as

$$C_T = C_L \sin(\alpha) - C_{Di}\cos(\alpha) \approx C_L\alpha - C_{Di} \qquad (19)$$

Substitution of Eqs. (10) and (13) yields

$$C_T = C_L\alpha\left[\tfrac{1}{2} + \tfrac{1}{3}\sin(\varepsilon)\right] = (\pi/2)\mathrm{AR}\alpha^2\left[1 - \tfrac{2}{3}\sin(\varepsilon)\right]\left[\tfrac{1}{2} + \tfrac{1}{3}\sin(\varepsilon)\right] \qquad (20)$$

In the limiting case as $\varepsilon \to 0$ deg, Eq. (20) reduces to

$$C_{T_{\varepsilon\to 0}} = (\pi/4)\mathrm{AR}\alpha^2 \qquad (21)$$

a result also indicated by SWT, which shows that the thrust is equal and opposite to the drag. Figure 3 presents C_T/α^2 as a function of AR. Equation (20) and numerical data are shown. The predictions show excellent accord with the panel method data, with only a small deviation at high AR, which is indicative that the spanwise loading is starting to deviate from elliptic. The close accord indicates that the extended SWT will closely estimate the performance (lift, drag, and pitching moment) of planar delta wings with attached leading-edge flow.

Also included in the presentation is the function $C_T/\alpha^2\cos(\Lambda)$. This expression can be interpreted as approximating Polhamus'[11] vortex lift constant Kv. Predictions of Kv using the Lamar–Gloss[7] panel method are shown, as are results from evaluation of the function. Agreement is seen to be excellent for AR < 4.

Many slender delta wings are designed with sharp leading edges such that they can benefit from lift augmentation due to the formation of conical leading-edge vortices. An accurate method to estimate the performance of this class of wings was devised by Polhamus[11] in the 1960s, his "leading-edge suction analogy." His methodology

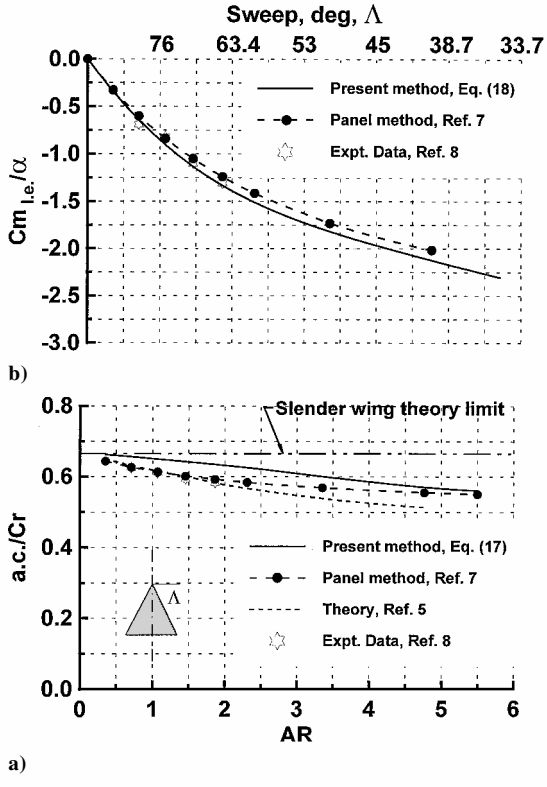

Fig. 2 a) Predicted a.c. location compared to numerical and experimental data and b) Predicted apex pitching moment compared to numerical and experimental data.

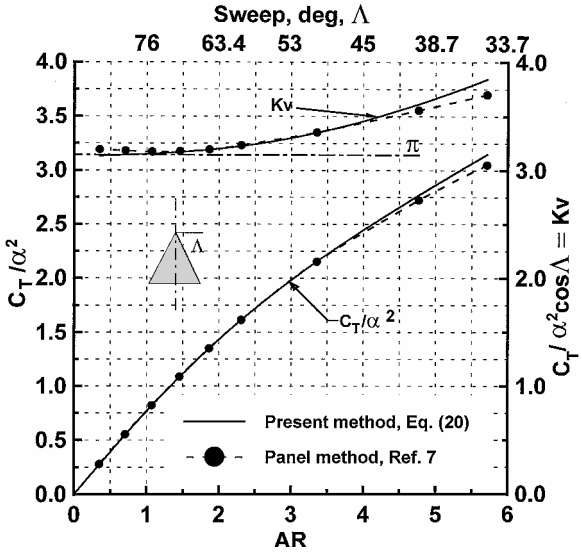

Fig. 3 Predicted leading-edge thrust coefficient compared to numerical data.

indicates that the lift produced by a thin, planar sharp-edged delta wing is closely approximated by

$$C_L = C_{L\alpha}\cos(\alpha)^2\sin(\alpha) + Kv\cos(\alpha)\sin(\alpha)^2 \qquad (22)$$

where the first term on the right represents the attached flow potential lift with zero leading-edge suction and the second term the vortex induced lift. Equation (22) generally shows excellent agreement with experimental data for AR < 2. As indicated, by use of the present methodology, Kv may be approximated as (Fig. 3)

$$Kv \approx \frac{\pi AR}{2\sin(\varepsilon)}\left[1 - \frac{2}{3}\sin(\varepsilon)\right]\left[\frac{1}{2} + \frac{1}{3}\sin(\varepsilon)\right] \qquad (23)$$

Thus, the present method [Eqs. (11) and (23)] in combination with Polhamus'[11] analogy may also be used to estimate the lift and drag $[=C_L\tan(\alpha)]$ of planar sharp-edged delta wings.

If the delta wing has a profiled section, the present results, in combination with the method presented in Ref. 12, may be used to estimate the lift and drag decomposition due to partial leading-edge flow separation.

Conclusions

A method is presented to extend the results from slender wing theory to delta wings of high aspect ratio. This incompressible technique is applicable to planar delta wings with fully attached leading-edge flows. A correction to account for the finite chord of the wing is incorporated into the rate of change of the local additional apparent mass. This expression contains a correction to account for the impact of wing sweep. Following the method of Jones,[1] simple expressions for the chordwise loading, lift, and coefficients including wing lift, induced drag, pitching moment, leading-edge thrust, as well as the a.c. location, are derived. Comparisons of these expressions with numerical and experimental data show excellent agreement.

Acknowledgement

The author would like to thank Murray Tobak for his comments.

References

[1]Jones, R. T., "Properties of Low-Aspect-Ratio Pointed Wings at Speeds Below and Above the Speed of Sound," NACA TN 835, 1946.

[2]Katz, J., and Plotkin, A., *Low-Speed Aerodynamics, From Wing Theory to Panel Methods*, 1st ed., McGraw–Hill, New York, 1991, pp. 212–222.

[3]Lawrence, H. R., "The Lift Distribution on Low-Aspect-Ratio-Wings at Subsonic Speeds," Cornell Aeronautical Lab. Rept. AF-673-A-1, Cornell Univ., Ithaca, NY, Aug. 1950.

[4]Lomax, H., and Sluder, L., "Chordwise and Compressibility Corrections to Slender-Wing Theory," NACA Rept. 1105, Nov. 1952.

[5]Traub, L. W., "Implications of the Insensitivity of Vortex Lift to Sweep," *Journal of Aircraft*, Vol. 37, No. 3, 2000, pp. 531–533.

[6]Kirkpatrick, D. L. I., "Analysis of the Static Pressure Distribution on a Delta Wing in Subsonic Flow," Aeronautical Research Council, A.R.C. R&M 3619, London, Aug.1970.

[7]Lamar, J. E., and Gloss, B. B., "Subsonic Aerodynamic Characteristics of Interacting Lifting Surfaces with Separated Flow Around Sharp Edges Predicted by a Vortex Lattice Method," NASA TN D-7921, Sept. 1975.

[8]Traub, L. W., "Effects of Spanwise Camber on Delta Wing Aerodynamics: An Experimental and Theoretical Investigation," Ph.D. Dissertation, Aerospace Engineering, Texas A&M Univ., College Station, TX, May 1999.

[9]Wentz, W. H., Jr., and Kohlman, D. L., "Wind Tunnel Investigations of Vortex Breakdown on Slender Sharp-Edged Wings," NASA CR 98737, Nov. 1968.

[10]Traub, L. W., "Prediction of Delta Wing Leading-Edge Vortex Circulation and Lift-Curve Slope," *Journal of Aircraft*, Vol. 34, No. 3, 1997, pp. 450–452.

[11]Polhamus, E. C., "A Concept of the Vortex Lift of Sharp-Edge Delta Wings Based on a Leading-Edge Suction Analogy," NASA TN D-3767, Oct. 1966.

[12]Traub, L. W., "Analytic Prediction of Lift for Delta Wings with Partial Leading-Edge Thrust," *Journal of Aircraft*, Vol. 31, No. 6, 1994, pp. 1426–1429.

Simple Engineering Model for Delta-Wing Vortex Breakdown

D. I. Greenwell*
University of Bristol,
Bristol, England BS8 1TR, United Kingdom

Introduction

THE leading-edge vortex flow structures generated by combat aircraft at high angles of attack continue to be the subject of much theoretical and experimental research. One aspect of these flows of particular concern is the onset of large-scale instabilities in the vortex (referred to as "burst" or "breakdown") because this impacts directly (and adversely) on aircraft performance, stability, and controllability. A wide range of theoretical mechanisms for this breakdown have been proposed,[1] all fundamentally based on stability analyses of an axisymmetric vortex. A common feature of all of these approaches is the emergence of the swirl ratio as the primary factor governing the onset of vortex breakdown. Further, despite the different assumptions made, the critical values obtained for the swirl ratio are remarkably similar (of the order of one) and agree reasonably well with experiment (e.g., Ref. 2). However, these theoretical analyses all fail to give any significant information about the structure of the vortex downstream of breakdown; unfortunately, it is just this aspect of the phenomenon that governs its impact on aircraft aerodynamic characteristics. Recent advances in computational fluid dynamics have led to the capability to reproduce helical vortex breakdown structures for delta-wing flows[3]; however, these computations are time consuming and expensive. This Note therefore presents some preliminary results from an alternative "engineering" analysis based on a very simple flow model, an analysis that gives quantitative predictions for the helical burst structure which compare well with experimental data.

Model Approach

The analysis builds on two main (but largely empirical) observations: 1) the structure of a burst delta-wing vortex is fundamentally helical,[4,5] and 2) during the transition from straight unburst vortex to helical burst vortex individual elements of the vortex core are initially deflected directly away from the vortex centerline and acquire no additional rotational velocity component.[4,6]

The burst process is then modelled as four stages, as illustrated in Fig. 1. Upstream of burst there is a semi-infinite straight vortex, followed by a deceleration stage ahead of the burst onset proper. In the region of the burst onset, there is a highly three-dimensional transition stage, leading into a semi-infinite helical vortex downstream of the burst region. This preliminary analysis does not address the complex flow physics of the initial burst development, but instead looks at the overall transformation from a columnar vortex (upstream) to a semi-infinite helical vortex (downstream). In some respects this is a similar approach to that adopted in Ref. 5; the critical difference being that in Ref. 5 the helical vortex geometry (i.e., orientation, pitch, and radius) was determined solely on the basis of experimental data.

For a right-handed helical vortex filament of strength Γ with viscous core radius σ, helix radius a_0, and pitch $p(=2\pi k)$, the

Received 17 June 2002; revision received 16 October 2002; accepted for publication 18 October 2002.

*Reader in Experimental Aerodynamics, Department of Aerospace Engineering; Doug.Greenwell@bristol.ac.uk.